Science of the Total Environment 633 (2018) 618–629

Contents lists available at ScienceDirect

Science of the Total Environment

journal homepage: www.elsevier.com/locate/scitotenv

Effects of increasing atmospheric CO_2 on the marine phytoplankton and bacterial metabolism during a bloom: A coastal mesocosm study

Yibin Huang [a,b], Xin Liu [a,b], Edward A. Laws [c], Bingzhang Chen [d], Yan Li [a], Yuyuan Xie [a,b], Yaping Wu [e], Kunshan Gao [a,*], Bangqin Huang [a,b,*]

[a] State Key Laboratory of Marine Environmental Science, Xiamen University, Xiamen, China
[b] Fujian Provincial Key Laboratory of Coastal Ecology and Environmental Studies, Xiamen University, Xiamen, China
[c] Department of Environmental Sciences, College of the Coast and Environment, Louisiana State University, Baton Rouge, LA, USA
[d] Ecosystem Dynamics Research Group, Research and Development Center for Global Change, Japan Agency for Marine-Earth Science and Technology, Yokohama, Japan
[e] College of Oceanography, Hohai University, Nanjing, China

HIGHLIGHTS

- The effects of increasing atmospheric CO_2 were assessed in a coastal mesocosm.
- CO_2 enrichment enhanced primary production and photosynthesis efficiency.
- Elevation of atmospheric CO_2 decreased bacterial respiration.
- CO_2 enrichment enhanced carbon transfer efficiency through the microbial loop.
- The contemporaneous responses have profound implications on carbon cycle.

GRAPHICAL ABSTRACT

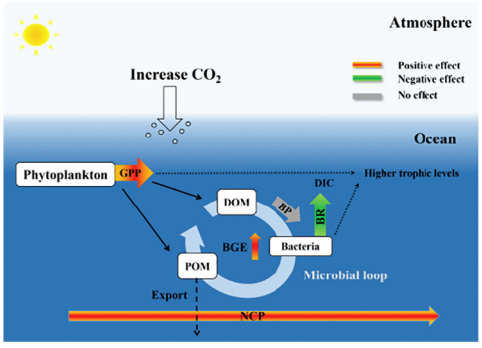

ARTICLE INFO

Article history:
Received 17 November 2017
Received in revised form 23 February 2018
Accepted 19 March 2018
Available online 28 March 2018

Editor: Daniel Wunderlin

Keywords:
CO_2 enrichment
Mesocosm scale
Gross primary production
Bacterial respiration
Bacterial growth efficiency
Net community production

ABSTRACT

Increases of atmospheric CO_2 concentrations due to human activity and associated effects on aquatic ecosystems are recognized as an environmental issue at a global scale. Growing attention is being paid to CO_2 enrichment effects under multiple stresses or fluctuating environmental conditions in order to extrapolate from laboratory-scale experiments to natural systems. We carried out a mesocosm experiment in coastal water with an assemblage of three model phytoplankton species and their associated bacteria under the influence of elevated CO_2 concentrations. Net community production and the metabolic characteristics of the phytoplankton and bacteria were monitored to elucidate how these organisms responded to CO_2 enrichment during the course of the algal bloom. We found that CO_2 enrichment (1000 μatm) significantly enhanced gross primary production and the ratio of photosynthesis to chlorophyll *a* by approximately 38% and 39%, respectively, during the early stationary phase of the algal bloom. Although there were few effects on bulk bacterial production, a significant decrease of bulk bacterial respiration (up to 31%) at elevated CO_2 resulted in an increase of bacterial growth efficiency. The implication is that an elevation of CO_2 concentrations leads to a reduction of bacterial carbon demand and enhances carbon transfer efficiency through the microbial loop, with a greater proportion of fixed carbon being allocated to bacterial biomass and less being lost as CO_2. The contemporaneous responses of phytoplankton and bacterial

* Corresponding authors at: State Key Laboratory of Marine Environmental Science, Xiamen University, Xiamen, China.
E-mail addresses: bqhuang@xmu.edu.cn (B. Huang), ksgao@xmu.edu.cn (K. Gao).

https://doi.org/10.1016/j.scitotenv.2018.03.222

metabolism to CO_2 enrichment increased net community production by about 45%, an increase that would have profound implications for the carbon cycle in coastal marine ecosystems.

1. Introduction

Increases of anthropogenic emissions of CO_2 since the Industrial Revolution are known to have influenced organisms and the delivery of oceanic ecosystem services at a global scale (Doney et al., 2009; Sampaio et al., 2018). Atmospheric pCO_2 has increased from the pre-industrial value of 280 μtam to the present-day value of ~400 μtam and is expected to further increase to 800–1000 μtam by the end of this century according to the "business as usual" CO_2 emission scenario (Stocker et al., 2013). Increasing dissolution of atmospheric CO_2 into the oceans leads to progressive ocean acidification (OA) and a shift in the distribution of inorganic carbon species in seawater (Caldeira and Wickett, 2003). The impacts of projected CO_2 emissions will likely induce a decrease of 0.3–0.4 in seawater pH by the end of this century (Gattuso et al., 2015). In coastal regions, the rate of decline of pH will likely be exacerbated by the interactions between OA and other natural or anthropogenic processes (Feely et al., 2010; Cai et al., 2011; Yu et al., 2017). In marine systems, phytoplankton and heterotrophic bacteria play a fundamental role in the carbon cycle; the former account for about half of global primary production (Behrenfeld and Falkowski, 1997), and the latter play a vital role in recycling nutrients and organic matter through the microbial loop (Del Giorgio and Cole, 2000). These two groups may be directly and indirectly affected by OA, with major implications for marine ecosystems and biogeochemical processes (Riebesell et al., 2013b).

Studies of the direct effects of OA on marine phytoplankton physiology and community composition have focused particularly on diatoms, coccolithophores, and cyanobacteria (reviewed by Dutkiewicz et al., 2015). The impacts of OA on phytoplankton metabolism are linked to two main processes: (1) energy savings due to down-regulation of CO_2-concentrating mechanisms (CCMs) under enhanced CO_2 and HCO_3^- availability (Hopkinson et al., 2011) and (2) increased demand for energy associated with maintenance of a constant intracellular pH as the extracellular pH declines (Pörtner and Farrell, 2008). Various studies have reported positive (Hein and SandJensen, 1997; Riebesell et al., 2007; Iglesias-Rodriguez et al., 2008), neutral (Tortell and Morel, 2002; Feng et al., 2009), and negative (Gao and Zheng, 2010; Rokitta and Rost, 2012) effects of elevated CO_2 on phytoplankton growth rates and photosynthesis.

Relatively few studies have addressed the effects of elevated CO_2 on the metabolism of bacteria compared to phytoplankton, and those studies have tended to focus on bacterial production (Liu et al., 2010). Heterotrophic bacterial activity is likely to be affected by changes in the supply of organic substrates associated with microalgal carbon fixation and exudation under elevated pCO_2 conditions (Rochelle-Newall et al., 2004; Grossart et al., 2006) and deceases of seawater pH (Teira et al., 2012; Bunse et al., 2016). For example, stimulation of bacterial production, especially production associated with particle-attached bacteria, has been reported at high pCO_2, presumably because of the formation of more phytoplankton-derived particles, which serve as sites for bacterial attachment (Grossart et al., 2006). In contrast, Coffin et al. (2004) have reported a reduction of bacterial production within a deep-sea community at low pH due to the negative effect of the low pH on cell integrity. However, to our knowledge, there have been few direct reports of the effects of OA on bacterial respiration, despite its important role in the carbon cycle. Teira et al. (2012) first examined the response of bacterial respiration to elevated CO_2 in a culture and reported a reduction of respiration. The authors speculated that this response may have been related to a reduction of energetic costs at high pCO_2 (1000 μatm); under these conditions the pH of the water (7.6) was similar to the intracellular pH of the bacteria (Teira et al., 2012). However, little response of bacterial respiration to elevated CO_2 has been reported in a natural bacterial community in the Artic Ocean (Motegi et al., 2013). Therefore, effects of increased CO_2/lowered pH on heterotrophic bacterial metabolism are perhaps variable.

In this study, we used three phytoplankton species—*Phaeodactylum tricornuntum*, *Thalassiosira weissflogii*, and *Emiliania huxleyi*—and the bacterial flora from the algal cultures to carry out a coastal-water mesocosm experiment. The three selected species of phytoplankton come from two important functional groups in the marine ecosystem. As model species their responses to OA have been widely studied in the laboratory (Dutkiewicz et al., 2015), and increasing attention has been paid to document their responses under more natural and fluctuating environmental conditions. The experimental design took into consideration the extensive database from laboratory studies and was intended to be an intermediate and necessary step between laboratory-scale research and studies of highly complex natural communities. Compared with relatively stable laboratory conditions, the environment in a mesocsom is closer to natural conditions that include multiple stressors, variations in solar radiation, and diurnal temperature cycles. The advantage of a large enclosure (i.e., 4400 L in this study) is the ability to maintain the system in a self-sustaining manner over a period as long as 20–30 days, substantially longer than is possible in relatively small enclosures. Large mesocosm experiments can extend over many generation times of the organisms in the microbiocenosis and can therefore facilitate studies of biochemical cycling within the system. Large mesocosms also offer the opportunity for cross-disciplinary collaboration in a single study, which may provide a more comprehensive understanding of the consequences of OA at the ecosystem level, especially during algal blooming periods. The dynamics of the dissolved inorganic (DIC) in the mesocosms was a function of the continuous supply of CO_2 via aeration, photosynthesis, and community respiration; it therefore mirrored the carbon system dynamics during natural algal blooms in coastal waters, where the DIC system is strongly influenced by biological processes and air-sea gas exchange. We hypothesized that 1) in nutrient-rich coastal waters, elevated pCO_2 might enhance phytoplankton primary production and that bacterial growth and heterotrophic activity (i.e., respiration) would consequently be stimulated and that 2) these responses might collectively lead to an increase of net community production because the phytoplankton were expected to be more responsive to CO_2 enrichment than the bacteria. To test these hypotheses, we investigated the effects of CO_2 enrichment on net community production and the metabolic characteristics of phytoplankton and heterotrophic bacteria in a coastal mesocosm.

2. Materials and methods

2.1. Experimental setup

The mesocosm experiment was conducted on a floating platform at the Facility for the Study of Ocean Acidification Impacts of Xiamen University (FOANIC-XMU, 24°31′48″ N, 118°10′47″ E, Fig. S1) in Wu Yuan Bay, Xiamen (Liu et al., 2017). The experiment lasted from 22 December 2014 (day 0 with respect to algal inoculation) to 24 January 2015. Six cylindrical transparent thermoplastic polyurethane (TUP, 0.9 mm thick) bags were set up and submerged in the seawater along the southern side of the platform. Each mesocosm was about 1.5 m in diameter and 3 m deep, with 0.5 m projecting above the seawater. The volumes of the enclosures below the sea surface and headspace above were approximately 4.4 m^3 and 0.8 m^3, respectively. The headspace of each

bag was sealed during the experiments, with the exception of sampling times and a few small holes that were left in the top of the mesocosm bags for gas exchange. In addition, the bags were covered by plastic domes to prevent rainfall and dust from entering and to minimize the likelihood of contamination. For each mesocosm bag, approximately 4400 L of natural seawater pumped from Wuyuan Bay was filtered through an ultrafiltration water purifier system (MU801-4T, Midea, China) equipped with 0.01-μm pore size cartridges (made in Germany). The filtration device was equipped with an automatic backwash system to avoid congestion. The pre-filtered water was then simultaneously allocated into each bag at the same flow rate within a period of 24 h. A known amount of NaCl solution was added to each bag to facilitate accurate determination of the volume of seawater in the bags based on the change of the salinity before and after salt addition (Czerny et al., 2013). The initial pCO_2 of the seawater in the bay was about 650 μatm (pH = 7.6) because of the active decomposition of allochthonous organic matter by microbes. We set up three replicates of two distinct CO_2 partial pressures to simulate atmospheric pCO_2 at present (400 μatm) and by the end of this century (1000 μatm). To simulate a low pCO_2 level (LC, 400 μatm), approximately 2 L of Na_2CO_3 solution (~100 μmol kg^{-1}) was added to the LC treatments to accelerate the equilibrium between ambient air and seawater (Albright et al., 2016). Meanwhile, an equal amount of Na_2CO_2 solution was added to the HC treatment to ensure that the total alkalinity was the same in both treatments. For the high pCO_2 treatment (HC, 1000 μatm), three bags were each supplemented with approximately 5 L of pre-filtered CO_2-saturated seawater (Riebesell et al., 2013a). Because the 5 L of CO_2-saturated seawater was only ~0.11% of the volume of seawater (~4400 L) in each mesocosm bag, the change in the total alkalinity of the HC treatment due to addition of the CO_2-saturated seawater was negligible. Throughout the experiment, air containing either 1000 μatm CO_2 (HC treatment) or 400 μatm CO_2 (LC treatment) was bubbled into the mesocosms via a CO_2 Enricher device (CE-100, Wuhan Ruihua Instrument & Equipment, China) at a flow rate of 4.8 L per minute. Three 13-cm-diameter air stone disks connected to 6-mm-diameter gas tubes were placed at the bottom of each bag to evenly disperse the air into the water column. The pore size of the air stones, 30–50 μm, was expected to produce bubbles with diameters of 0.40–0.45 mm (Parthasarathy and Ahmed, 1996) that would rise at rates of 0.09–0.11 m s^{-1} (Martínez and Casas, 2012). We assumed that direct injection of these small bubbles through the air stone disk would not alter mixing effects or disturb the plankton in the mesocosm. We inoculated the mesocosms with phytoplankton species that had been studied extensively in the laboratory: two diatoms, *Phaeodactylum tricornuntum* (CCMA 106) and *Thalassiosira weissflogii* (CCMP 102), and the coccolithophorid *Emiliania huxleyi* (CS-369). Before being introduced into the mesocosms, the three phytoplankton species and their associated bacteria were cultured in autoclaved, pre-filtered seawater from Wuyuan Bay at 16 °C (similar to the in situ temperature of Wuyuan Bay) without any addition of nutrients. Cultures were continuously aerated with filtered ambient air containing 400 μatm of CO_2 within plant CO_2 chambers (HP1000G-D, Wuhan Ruihua Instrument & Equipment, China) at a constant bubbling rate of 300 mL min^{-1}. The culture medium was renewed every 24 h to maintain the cells of each phytoplankton species in exponential growth. The maximum quantum yield (F_v/Fm) of the three cultures was approximately 0.610 ± 0.005. F_v/Fm was calculated as $F_v/F_m = (F_m - F_0) / F_m$; where F_0 indicates the basal fluorescence under an irradiance of 0.2 μmol photons m^{-2} s^{-1} and F_m represents the maximal fluorescence measured with a saturating light pulse of 5000 μmol photons m^{-2} s^{-1} (0.8 s) for dark-adapted (10 min) samples. The initial concentrations of *Phaeodactylum tricornuntum*, *Thalassiosira weissflogii*, and *Emiliania huxleyi* inoculated into the mesocosm were 10, 10, and 20 cells mL^{-1}, respectively. The initial diatom/coccolithophorid cell ratio was therefore 1:1. We note that there were substantial differences in the cell sizes and the cellular chl-*a* contents of the three species. The cell sizes of the three species were roughly 20, 100, and 2000 μm^3 for *Emiliania huxleyi*, *Phaeodactylum tricornuntum*, and *Thalassiosira weissflogii*, respectively (Mullin et al., 1966; Strathmann, 1967). Correspondingly, the cellular chlorophyll *a* contents were approximately 0.14, 0.32, and 0.28 pg $cell^{-1}$ for these three species (Mullin et al., 1966; Strathmann, 1967). These differences could have affected competition for inorganic nutrients, CO_2, and light (Harris et al., 1983; Riebesell et al., 1993; Kerimoglu et al., 2012). However, we did not try to take cell size considerations into account in choosing the initial inoculum of each species because factors other than cell size can be major determinants of the outcome of species competition (Eppley, 1972; Legrand et al., 2003). Instead, we chose to begin the experiment with very low and equal concentrations of diatom and coccolithophore cells and assumed that after many generation times the best competitor would come to dominate the culture. Before the inoculations, no meaningful numbers of bacteria were counted by flow cytometer in the pre-filtered seawater. Bacteria associated with the algal cultures were also introduced into the mesocosm along with the phytoplankton assemblages. The initial bacterial assemblages were dominated by class Alphaproteobacteria, Gammaproteobacteria, and Flavobacteriia. No significant differences of bacterial assemblages between the HC and LC treatments were detected during the bloom (Lin et al., 2018). Based on the assessment by Riebesell et al. (2010) that an acclimation period of 8 generation times is sufficient for a study of ocean acidification effects on marine microorganisms, the ultra-low cell density at the beginning of the experiment ensured that all species (including bacteria) would be fully acclimated before the biomass was high enough to be detected. Over the course of the experiment, no zooplankton were found during microscopic examinations of the cultures for phytoplankton species.

2.2. Environmental parameters

The temperature and salinity of the mesocosms were measured with a conductivity-temperature-depth sensor (RBR, Canada). Chemical parameters including pH, total alkalinity, DIC, dissolved organic carbon, and nutrients were measured every two days (M. Dai, unpublished data.). Values of pH_T (pH on the total scale) were measured with the pH indicator meta-cresol purple with a spectrophotometer (Agilent 8453). This method is accurate to within ±0.0005 (Zhang and Byrne, 1996). The DIC concentration was determined with a CO_2 analyzer (LI 7000, Apollo SciTech, USA), as described by Cai et al. (2004). Total alkalinity was determined by Gran titration. Reference materials from the laboratory of Andrew Dickson (CRM Batch 60#) were used to calibrate the system to a precision of ±2 μmol kg^{-1} for DIC and total alkalinity (Cai et al., 2004). The pCO_2 was calculated from the measured DIC and pH_T with the CO_2Sys Program (Pierrot et al., 2006) using the stoichiometric equilibrium constants for carbonic acid of Mehrbach et al. (1973) as refitted in different functional forms by Dickson and Millero (1987).

2.3. Chlorophyll a

Chlorophyll *a* (chl-*a*) concentrations were measured by high-performance liquid chromatography (HPLC) with a Shimadzu 20A HPLC system fitted with a 3.5-μm Eclipse XDB C_8 column (4.6 × 150 mm, Agilent Technologies, Waldbronn, Germany). Details of the procedure have been described by Liu et al. (2015). Briefly, samples for phytoplankton pigment analysis (0.2–2 L, according to biomass) were filtered through 25-mm GF/F glass fiber filters under a vacuum pressure of <75 mm Hg and in dim light. The filters were then immediately frozen (−80 °C) until analysis in the laboratory (within 30 days). Phytoplankton pigments were extracted with *N*, *N*-dimethylformamide and analyzed with standards (DHI Water & Environment, Hørsholm, Denmark).

2.4. Abundance of unattached bacteria

Water samples (1.8 mL) for determination of cell numbers of unattached bacteria were collected from each bag, immediately fixed with 1% (final concentration) paraformaldehyde, and stored at −80 °C until analysis. Bacterial abundance was quantified using an Accuri C6 flow cytometer (Becton, Dickinson, USA) under a 488-nm laser after staining with fluorochrome SYBR-Green 1 (Marie et al., 1997). Fluoresbrite carboxy YG 1.0-μm diameter microspheres were also added to the samples as an internal standard for the quantification of cell concentrations. Milli-Q water was used as a sheath fluid, and the event rate was between 100 and 400 cells mL^{-1} to avoid coincidence. Data acquisition and analysis were conducted with BD Accuri C6 Software (Becton, Dickinson, USA).

2.5. In vitro oxygen-based microbial metabolism

Microbial metabolism was calculated from the changes of dissolved oxygen concentrations before and after 24-h incubations (Serret et al., 1999). The dissolved oxygen concentration was measured by high-precision Winkler titration (Metrohm-848, Switzerland) for detection of the potentiometric end-point (Oudot et al., 1988). Water samples collected from each bag were transferred to 5-L polycarbonate bottles with a silicone tube and subsequently siphoned into calibrated 60-cm^3 borosilicate bottles. Initial oxygen concentrations were measured at the start of the incubations. Two sets of three light and three dark incubation bottles were placed in a large tank filled with water exposed to natural sunlight. The incubation temperature was maintained by running seawater. Gross primary production (GPP) was equated to the difference between the average dissolved oxygen concentrations in the light and dark bottles at the end of the incubations; community respiration (CR) was equated to the difference between the average dissolved oxygen concentrations in the initial and dark bottles. Measured GPP based on incubations in the large tank were assumed to be light-saturated rates (hereafter GPP_m). Estimates of in situ, depth-averaged gross primary production ($GPP_{in\text{-}situ}$) were made on the assumption that photosynthetic rates were a hyperbolic function of irradiance and the attenuation of light with depth was due to the absorption by phytoplankton pigments (Supporting Information). Net community production (NCP) was equated to the difference between $GPP_{in\text{-}situ}$ and CR.

The respiration rates of the unattached bacteria were estimated using water that had been pre-filtered (0.8 μm Nuclepore filter, Millipore) at a low negative pressure. The filtered water was dispensed into two sets of initial and dark bottles. The respiration rates of the unattached bacteria were equated to the difference between the average dissolved oxygen concentrations in the initial bottle and the dark bottle containing 0.8-μm–pre-filtered water. Large-size respiration ($R_{>0.8\mu m}$) was equated to the difference between CR and the respiration rates of the unattached bacteria. We assumed that $R_{>0.8\mu m}$ was the sum of the respiration rates of the phytoplankton (PR) and attached bacteria because virtually no zooplankton passed through the ultrafiltration water purifier. The PRs were assumed to be a constant percentage of the corresponding gross photosynthetic rates on the assumption that PR was directly proportional to rates of photosynthesis (Laws and Caperon, 1976; Laws and Bannister, 1980) and the fact that the phytoplankton populations that bloomed in the mesocosms were dominated by *Phaeodactylum tricornuntum* (Liu et al., 2017). It was necessary that PR as a percentage of gross photosynthesis lie between 0% and 4.8% in the LC treatment and between 0% and 7.4% in the HC treatment to assure that the estimated respiration rates of the phytoplankton and attached bacteria were not negative in the two treatments on any day. These upper limits (4.8% in the LC treatment and 7.4% in the HC treatment) were estimated from the ratio of $R_{>0.8\mu m}$ to $GPP_{in\text{-}situ}$ on the day when that percentage was a minimum (day 11 for the LC treatment and day 9 for the HC treatment), when we assumed that the respiration rates of the attached bacteria were negligible compared to PR. We evaluated the impact of varying the assumed percentages on the patterns of bulk bacterial respiration and bacterial growth efficiency (Supporting Information). The results showed that the differences between bulk bacterial respiration and bacterial growth efficiency in the two treatments were statistically significant ($p \le 0.05$) when the assumed percentages were larger than 1.3% in both treatments (Table S1). In the present study, the assumed fractions of PR (4.8% in the LC treatment and 7.4% in the HC treatment) were adopted. These estimated percentages of PR in the LC and HC treatments are very comparable to the results for *Phaeodactylum tricornuntum* under similar pCO_2 conditions reported by Li et al. (2017). The difference between $R_{>0.8\mu m}$ and PR was then equated to the respiration rates of the attached bacteria. Bulk bacterial respiration (BR) was then equated to the sum of the respiration rates contributed by both attached and unattached bacteria. The relative contributions of attached and unattached bacteria to bulk BR found in this study are very consistent with a previous report by Smith et al. (1995), who found that diatoms were colonized by bacteria throughout a diatom bloom in a mesocosm, and attached bacteria contributed about 70% of the bulk BR during the stationary phase.

Changes of oxygen concentrations in triplicate incubation bottles collected from the same mesocosm were averaged to calculate the metabolic rate of one subsample. Rates of three subsamples from similar pCO_2 treatments were then combined to calculate the median value and median absolute deviation for each sample day. In total, we had 96 estimates of each rate for the two treatments during the 16 sampling days. Oxygen-based metabolism was converted to a carbon basis using a respiratory quotient of 0.9 on the assumption that inorganic nitrogen was released from organic matter in the form of ammonium (Laws, 1991; Hedges et al., 2002).

2.6. Bulk bacterial production

Bulk bacterial production (BP) was determined with the ^3H-leucine incorporation method (Kirchman, 1993). Four 1.8-mL aliquots of water were collected from each bag, added to 2-mL sterile microcentrifuge tubes (Axygen, Inc., USA), and incubated with a saturating concentration (10 nmol L^{-1}) of L-[3,4,5-^3H(N)]-Leucine (Perkin Elmer, USA) for 2 h in the dark. One sample was immediately killed by adding 100% trichloroacetic acid (TCA) as a control, and the other three were terminated with TCA at the end of the 2-h incubation. The water samples were filtered onto 0.2-μm polycarbonate filters (GE Water & Process Technologies, USA). The filters were rinsed twice with 3 mL of 5% TCA and twice with 2 mL of 80% ethanol before being frozen at −20 °C. Upon return to the laboratory, the dried filters were placed in scintillation vials with 5 mL of Ultima Gold scintillation cocktail (Perkin-Elmer, USA). Radioactivity retained on the filters was measured as disintegrations per minute using a Tri-Carb 2800TR liquid scintillation counter (Perkin Elmer, USA). The rate of incorporation of ^3H leucine was calculated from the difference between the activities of the treatment and control tubes. We used a factor of 1.5 kg C mol $leucine^{-1}$ to convert the incorporation of leucine to carbon equivalents, assuming no isotopic dilution (Kirchman, 1993). Bacterial carbon demand (BCD) was equated to bulk BP + bulk BR, and bacterial growth efficiency (BGE) was equated to bulk BP /BCD (Motegi et al., 2013).

2.7. Statistical analyses

Two-sided Student's *t*-tests were used to determine whether average growth rates were significantly different from zero and to distinguish the different growth phases. Effects of CO_2 enrichment were tested by repeated-measures analysis of variance (ANOVA) with time as a within-subject factor and pCO_2 (two levels) as the between-subject factor during the different phases of the algal bloom. If the assumption of equal between-group correlation and variance ("sphericity") was violated (Mauchly's test, $p < 0.05$), a Huynh–Feldt correction was applied. Significant differences were judged if the type I error rate

(p) was <0.05. All statistical analyses were performed using SPSS (SPSS software, SPSS Inc., Chicago, USA).

3. Results

3.1. Initial conditions and algal bloom development

During the study period, water temperatures deviated by <1 °C from a mean of 16 °C (Table 1), and the water in each bag was well mixed. Initial nitrate ($NO_2^- + NO_3^-$), ammonium (NH_4^+), phosphate (PO_4^{3-}), and silicate (SiO_3^{2-}) concentrations were 52–54 μmol L^{-1}, 20–21 μmol L^{-1}, 2.4–2.6 μmol L^{-1}, and 38–41 μmol L^{-1}, respectively (Table 1). The total alkalinity values in the seawater were 2480 ± 56 μmol kg^{-1} (mean value ± standard deviation, the same below) and 2470 ± 27 μmol kg^{-1} in the HC and LC treatments, respectively, on day 0. The pCO_2 of the seawater was higher in the HC treatment (1220 ± 150 μatm) than in the LC treatments (390 ± 54 μatm) initially (Fig. 1a). Because of the high rates of bacterial respiration, the pCO_2 values increased (by approximately 300 μatm) during the first few days in both treatments (Fig. 1a). Although air containing 1000 μatm CO_2 was continuously bubbled into the HC treatments, the pCO_2 values in both treatments decreased after day 6 because of rapid CO_2 uptake by the phytoplankton and were no longer different between the two treatments by day 16 (Fig. 1a). Similar to the pCO_2 time series, the temporal variation of pH_T was driven by the high rates of biological activity. There was an initial decline in pH_T due to bacterial respiration and a subsequent increase as algal blooms developed (Fig. 1a). In all the mesocosms, the development of an algal bloom led to a rapid decrease of nutrients. The nitrate concentrations dropped to very low levels of approximately 2.8 ± 0.3 μmol L^{-1} in the LC treatment and 5.8 ± 6.1 μmol L^{-1} in the HC treatment on day 15 (Table 1). At the end of the study, both phosphate and nitrate concentrations were close to their limits of detection (Table 1). The initial DIC was higher in the HC treatment (2321 ± 5.8 μmol kg^{-1}) than in the LC treatment (2163 ± 24 μmol kg^{-1}) (Table 1). The DIC, like the pCO_2, increased in the first few days and then decreased as the algae grew (Table 1)

After inoculation, phytoplankton pigment biomass in terms of chl-*a* increased rapidly (Fig. 1b). The chl-*a* concentrations reached peaks of 385 ± 5.3 μg L^{-1} and 364 ± 31 μg L^{-1} in the LC (day 17) and HC (day 21) treatments, respectively (Fig. 1b). Based on growth rates calculated from the natural logarithms of the chl-*a* concentrations and measured rates of photosynthesis and physiological performance (i.e., light-saturated productivity indices), two growth phases were initially identified: (1) log phase (days 0–12), when average phytoplankton growth rates were significantly greater than zero (0.7 ± 0.2 d^{-1} in the LC treatment and 0.7 ± 0.3 d^{-1} in the HC treatment, $p = 0.001$, t-test) and before the decline of the light-saturated productivity indices in the two treatments (Figs. 1b and 2b); and (2) stationary phase (days 13–34), when average growth rates (0.0 ± 0.2 d^{-1} in the LC and − 0.0 ± 0.3 d^{-1} in the HC treatment) were not significantly different from zero ($p = 0.749$, t-test. Fig. 1b). The stationary phase was further divided into two phases: stationary phase I (days 13–22) and stationary phase II (days 23–34). During stationary phase II light-saturated productivity indices were relatively constant after declining during stationary phase I (Fig. 2b). Initial abundances of the unattached bacteria averaged 7.7 ± 0.7 × 10^6 cells μL^{-1} and 7.6 ± 0.1 × 10^6 cells μL^{-1} in the LC and HC treatments, respectively (Fig. 1c). Thereafter, the abundances of the unattached bacteria dramatically decreased to minimal values on day 9 (Fig. 1c), by which time phytoplankton populations had increased by roughly a factor of 400 (Fig. 1b). Throughout the stationary phase, both chl-*a* concentrations and the abundances of the unattached bacteria remained relatively constant in the two treatments

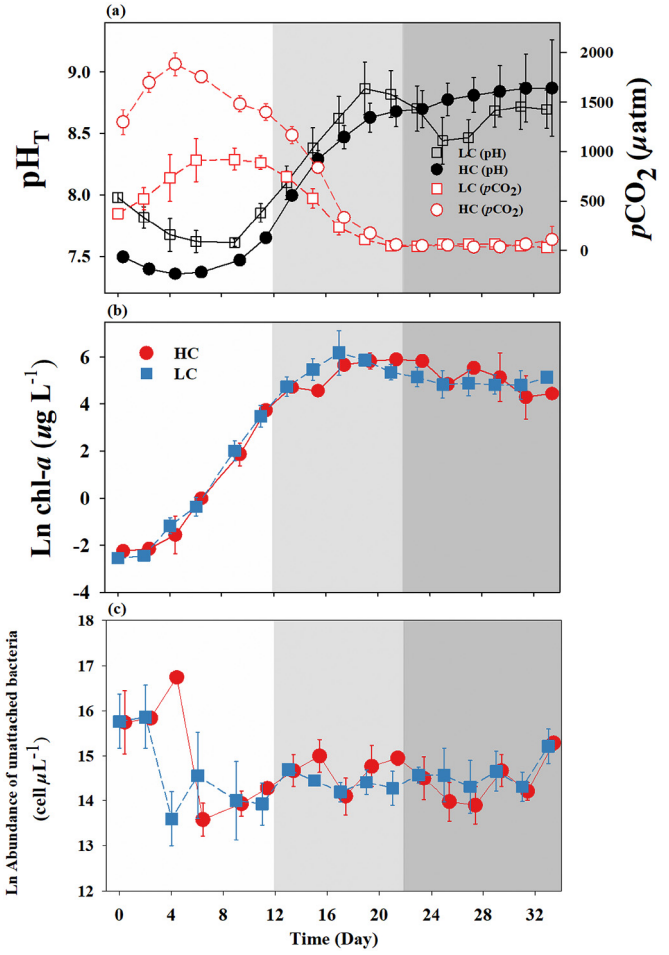

Fig. 1. Temporal variations of (a) pCO_2 and pH_T in the seawater, (b) chlorophyll *a* (chl-*a*) and (**c**) abundance of the unattached bacteria in the high pCO_2 level (HC) and low pCO_2 level (LC) treatments. White, light grey and dark grey shaded area indicate the log phase, stationary phase I and stationary phase II of the algae bloom, respectively. Data are mean ± standard deviation; $n = 3$.

Table 1
Summary of environmental characteristics of the mesocosms over the course of experiment.

		Temp	Salinity	$NO_3^- + NO_2^-$	NH_4^+	PO_4^{3-}	SiO_3^{2-}	DIC	pH_T	pCO_2
		°C		μmol L^{-1}	μmol L^{-1}	μmol L^{-1}	μmol L^{-1}	μmol kg^{-1}		(μatm)
Day 0	LC	15	29	52–56	19–23	2.4–2.8	38–40	2143–2163	8.0	1170–1284
	HC	15	29	51–55	19–23	2.3–2.7	38–39	2315–2320	7.5	370–413
Log phase I	LC	15–16	29	15.0–52	1.6–20	0.5–2.6	31–38	1825–2178	7.9–8.4	373–888
(Days 1–12)	HC	15–16	29	47–54	0.2–21	0.7–2.5	34–39	2029–2338	7.4–8.2	1295–1396
Stationary phase I	LC	15–16	29	~15.9	-	0.1–0.5	10–24	1706–1745	8.4–8.5	46–749
(Days 13–22)	HC	15–16	29	1.1–25	-	~0.1	29–30	1740–1891	8.4–8.6	59–1164
Stationary phase II	LC	15–16	29	-	-	-	10–16	1673–1706	8.5–8.8	30–43
(Days 22–33)	HC	15–16	29	-	-	~0.3	24–25	1616–1740	8.6–8.7	34–110

Notes: The pH_T changes were measured with a pH indicator meta-cresol purple with a spectrophotometer. "-" means the values were below the detection limit
HC: high pCO_2 level treatment. LC: low pCO_2 level treatment. Tem: temperature. DIC: dissolved inorganic carbon.

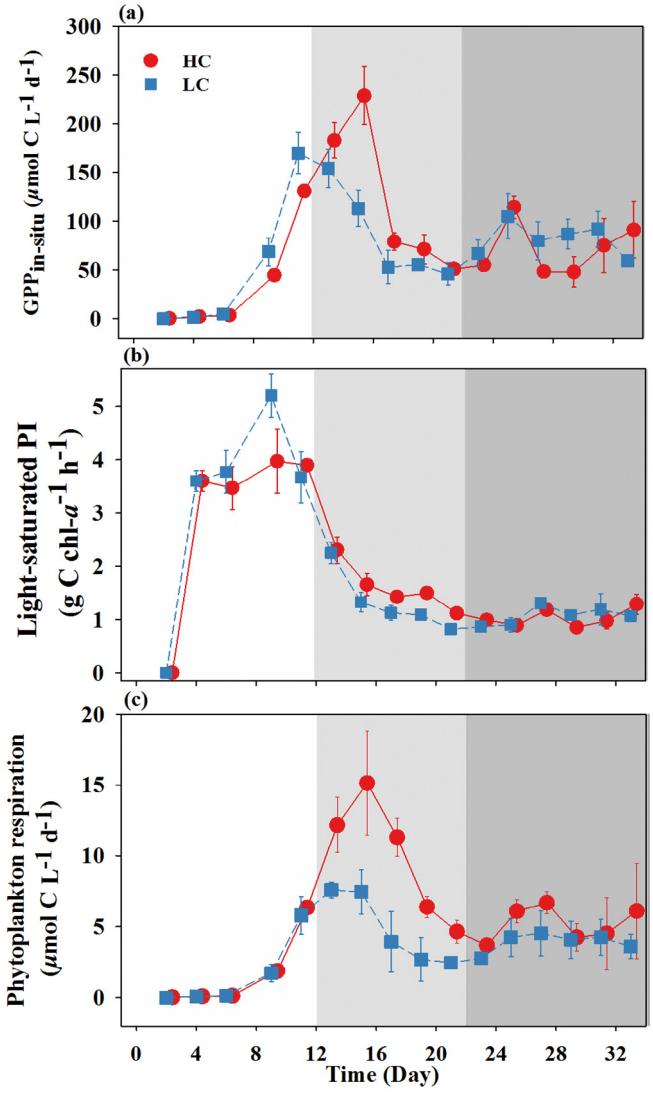

Fig. 2. Temporal variations of (a) in situ, depth-averaged gross primary production ($GPP_{in\text{-}situ}$), (b) light-saturated productivity indices (PI, light-saturated GPP/chlorophyll *a*) (c) estimated phytoplankton respiration in the high pCO_2 level (HC) and low pCO_2 level (LC) treatments. White, light grey and dark grey shaded area indicate the log phase, stationary phase I and stationary phase II of the algae bloom, respectively. Data are median ± median absolute deviation; n = 3.

(Fig. 1b,c). No consistent differences between the abundances of the unattached bacteria and chl-*a* concentrations were apparent between the two treatments during either of the growth phases (Table 2).

3.2. Autotrophic metabolism

$GPP_{in\text{-}situ}$ increased rapidly during the algal bloom and declined during the stationary phase (Fig. 2a). Maxima of $GPP_{in\text{-}situ}$ were recorded near day 14 (Fig. 2a). During stationary phase I, daily $GPP_{in\text{-}situ}$ in the HC treatment was 38% greater than in the LC treatment ($p = 0.021$; Table 2). During stationary phase II, there was no significant difference between $GPP_{in\text{-}situ}$ in the HC and LC treatments (Fig. 2a; Table 2). Productivity indices (i.e., the ratio of light-saturated GPP to chl-*a*) increased dramatically during the first few days of log-phase growth and reached maxima of roughly 5.3 g C g^{-1} chl-a^{-1} h^{-1} (Fig. 2b). However, productivity indices declined rapidly during stationary phase I and were <1 g C g^{-1} chl-a^{-1} h^{-1} throughout stationary phase II, an indication of extreme light and/or nutrient limitation (Fig. 2b). During stationary phase I, productivity indices in the HC treatment were 39% higher than in the LC treatment for a period of 10 days ($p = 0.027$; Table 2).

3.3. Heterotrophic bacterial metabolism

Bulk BP increased threefold from the log phase to stationary phase I and even further during stationary phase II (Fig. 3a). There was no significant difference between bulk BP in the LC and HC treatments (Table 2). Similar to the trend of bulk BP, bulk BR increased by about a factor of four between the log phase and stationary phase (Fig. 3b, c), but in the case of bulk BR, there was a significant difference in the LC and HC treatments throughout stationary phase I ($p = 0.024$; Table 2). Bulk BR was about 31% lower in the HC treatment during that time (Fig. 3c). During the log phase, the attached and unattached bacteria accounted for roughly equal amounts of bulk BR, but during the stationary phase attached bacteria accounted for about 78% of bulk BR (Fig. 3b). Similar to the response of bulk BR to the elevated CO_2 concentrations, the respiration rates of attached and unattached bacteria were significantly lower in the LC treatment during days 13–22 ($p = 0.030$ for the respiration rates of attached bacteria and $p = 0.021$ for the respiration rates of attached bacteria; Table 2). BGE was relatively low (<5%) during the first eight days of the experiment and then increased until day 16 (Fig. 4a). During days 13–22, BGEs were significantly higher in the HC treatment than that in the LC treatment ($p = 0.030$; Table 2). There was no consistent difference in BGEs between the two treatments during the log phase and stationary phase II (Table 2). In contrast, the BCD was about 30% lower in the HC treatment than in the LC treatment during days 13–22 ($p = 0.027$; Table 2). The BCD remained low during the start of the experiment and increased due to the elevations of bulk BP and bulk BR (Fig. 4b).

3.4. Community respiration and metabolic balance

The $R_{>0.8\mu m}$ (Fig. 5a), which includes the respiration rates of both the phytoplankton and particle-attached bacteria, was significantly correlated with chl-*a* ($r = 0.83$, $p < 0.001$). During the stationary phase, it was relatively stable in the range 46–65 μmol C L^{-1} d^{-1} (Fig. 5a). There was no significant difference in $R_{>0.8\mu m}$ between the two treatments (Table 2). Bulk BR accounted for a majority of CR in both treatments, but the contribution of bulk BR to CR was lower in the HC treatment than in the LC treatment (Figs. 3b, 5b). Like bacterial abundance, CR trended down until day 9 (Fig. 5b). It then began to increase with the growth of phytoplankton until the end of sampling (Fig. 5b). There was no significant difference in CR between the two treatments (Table 2).

In general, the temporal pattern of NCP was similar to that of $GPP_{in\text{-}situ}$ but offset by the contributions of CR (Fig. 5c). NCP was negative (i.e., community metabolism was heterotrophic) for roughly the first week and last two weeks of the experiment (Fig. 5c). On day 6, NCP became positive and peaked around days 14–16 (Fig. 5c). Daily NCP was 45% higher in the HC treatments than in the LC treatments during stationary phase I ($p = 0.027$; Table 2).

4. Discussion

4.1. Algal bloom development and inorganic carbon system

This mesocosm study was conducted in the context of eutrophic coastal water, characterized by addition of an artificial assemblage previously studied extensively in the laboratory, and aimed to link the effects of OA in laboratory-based experiments with mesoscale studies. Whereas the diversity of the artificial assemblage differed from that of a natural community and whereas zooplankton were absent in the mesocosm, the relatively small number of species in the mesocosm facilitated assessment of the responses of the phytoplankton and their associated bacterial community to CO_2 enrichment in the absence of a complex community succession and trophic cascade. The experiment thereby provided a good opportunity to determine whether these

Table 2
Statistical analyses using repeated-measures analysis of variance (ANOVA) with time as a within-subject factor and pCO_2 (two levels) as the between-subject factor during the different phases of the algal bloom.

		Log phase	Stationary phase	
		Days 0–12	Days 13–22	Days 23–33
Chlorophyll *a*	Day	**0.008, df = 4**	0.116, df = 4	0.128, df = 5
	Day * pCO_2	0.412, df = 4	0.225, df = 1	0.467, df = 5
	pCO_2	0.445, df = 1	0.913, df = 4	0.551, df = 1
Abundance of unattached bacterial	Day	0.172, df = 4	0.782, df = 4	0.080, df = 5
	Day * pCO_2	0.443, df = 4	0.192, df = 1	0.221, df = 5
	pCO_2	0.607, df = 1	0.200, df = 4	0.983, df = 1
Gross primary production (in-situ)	Day	**0.001, df = 4**	**0.026, df = 4**	0.225, df = 5
	Day * pCO_2	0.755, df = 4	0.477, df = 4	0.364, df = 5
	pCO_2	0.485, df = 1	**0.021, df = 1**	0.525, df = 1
Light-saturated productivity indices	Day	0.138, df = 4	**0.027, df = 4**	0.359, df = 5
	Day * pCO_2	0.473, df = 4	0.339, df = 4	0.412, df = 5
	pCO_2	0.650, df = 1	**0.027, df = 1**	0.764, df = 1
Bulk bacterial production	Day	**0.01, df = 4**	0.345, df = 4	0.050, df = 5
	Day * pCO_2	0.755, df = 4	0.638, df = 4	0.012, df = 5
	pCO_2	0.568, df = 1	0.855, df = 1	0.893, df = 1
Bulk bacterial respiration	Day	**0.016, df = 4**	0.247, df = 4	0.654, df = 5
	Day * pCO_2	0.306, df = 4	0.474, df = 4	0.197, df = 5
	pCO_2	0.724, df = 1	**0.024, df = 1**	0.323, df = 1
Respiration of the attached bacteria	Day	0.185, df = 4	0.372, df = 4	0.118, df = 5
	Day * pCO_2	0.459, df = 4	0.446, df = 4	0.619, df = 5
	pCO_2	0.500, df = 1	**0.030, df = 1**	0.611, df = 1
Respiration of the unattached bacteria	Day	0.058, df = 4	0.256, df = 4	0.470, df = 5
	Day * pCO_2	0.504, df = 4	0.499, df = 4	0.487, df = 5
	pCO_2	0.514, df = 1	**0.021, df = 1**	0.800, df = 1
Bacterial growth efficiency	Day	**0.016, df = 4**	0.219, df = 4	0.642, df = 5
	Day * pCO_2	0.311, df = 4	0.447, df = 4	0.174, df = 5
	pCO_2	0.689, df = 1	**0.030, df = 1**	0.301, df = 1
Bacterial carbon demand	Day	**0.029, df = 4**	0.199, df = 4	0.484, df = 5
	Day * pCO_2	0.514, df = 4	0.316, df = 4	0.848, df = 5
	pCO_2	0.982, df = 1	**0.027, df = 1**	0.242, df = 1
Respiration of organism larger than 0.8 μm	Day	**0.006, df = 4**	0.146, df = 4	0.473, df = 5
	Day * pCO_2	0.070, df = 4	0.311, df = 4	0.495, df = 5
	pCO_2	0.205, df = 1	0.915, df = 1	0.265, df = 1
Community respiration	Day	**0.029, df = 4**	0.199, df = 4	0.484, df = 5
	Day * pCO_2	0.514, df = 4	0.316, df = 4	0.848, df = 5
	pCO_2	0.982, df = 1	0.683, df = 1	0.242, df = 1
Net community production	Day	**0.001, df = 4**	**0.028, df = 4**	0.270, df = 5
	Day * pCO_2	0.444, df = 4	0.423, df = 4	0.321, df = 5
	pCO_2	0.661, df = 1	**0.027, df = 1**	0.459, df = 1

Notes: Significant effects are in bold ($p < 0.05$).

species responded similarly in the laboratory and under more realistic environmental conditions.

The algal bloom in the mesocsoms developed rapidly, and *Phaeodactylum tricornutum*, which outcompeted *Thalassiosira weissflogii* and *Emiliania huxleyi*, accounted for >99% of the biomass during the stationary phase in the two treatments (Liu et al., 2017). The growth of algae consumed the nutrients rapidly in the enclosures, and the systems began to be subject to nutrient limitation as it entered stationary phase (Table 1). Unlike the comparatively small influence of biological processes on the inorganic carbon system in the open ocean, biological activity in nutrient-rich coastal seawater can have an impact on the inorganic carbon system that exceeds the rate of air-sea CO_2 exchange. At the start of the experiment, bacterial metabolism was strong due to the high dissolved organic carbon concentrations in the seawater and transformed much of the dissolved organic carbon into DIC, the result being a decrease in pH_T in both treatments (Fig. 1a). After that time, with the development of the algal bloom, photosynthesis was the dominant process impacting the inorganic carbon system. The pH_T gradually increased and reached 8.7 in the end of experiment (Fig. 1a). In coastal areas, elevated pH in seawater during a bloom is an often observed phenomenon due to the very rapidly photosynthetic fixation of CO_2, the result being that aquatic CO_2 concentration became much lower than atmospheric concentration (e.g. Seitzinger, 1991; Pinckney et al., 1997; Jacoby et al., 2000). This pattern would still be evident with an atmospheric pCO_2 of either 1000 or 2000 μatm. In our study, the most significant difference between the LC and HC treatment was the continuous supply of two levels of air containing 1000 μatm CO_2 (HC treatment) and 400 μatm CO_2 (LC treatment) over the course of the experiment. These two CO_2 supply rates acted as different forcing functions during the evolution of the blooms.

4.2. Responses of autotrophic metabolism

The effects of CO_2 fertilization on phytoplankton were most apparent during stationary phase I when *Phaeodactylum tricornuntum* dominated in the two treatments (Liu et al., 2017). We found a stimulation of $GPP_{in\text{-}situ}$ in the HC treatment (Table 2; Fig. 2a), which is consistent with the observation of enhanced ^{14}C-based net primary production and particulate organic matter accumulation during stationary phase I (Liu et al., 2017). The significantly higher productivity indices in the HC treatment during stationary phase I (Table 2; Fig. 2b) imply that the elevated primary production was due mainly to an increase in the efficiency of photosynthesis per chl-*a*. Effects of OA on *Phaeodactylum tricornuntum* have been extensively conducted in the laboratory. Most of those studies have been carried out under conditions of constant pCO_2 levels and abundant nutrients and light (see the review by Gao and Campbell, 2014). Several studies have reported that under controlled conditions increases of atmospheric CO_2 may have little effect on primary production because *Phaeodactylum tricornuntum* has an active CCM to take up both CO_2 and bicarbonate for photosynthesis to counteract the limited availability of CO_2 in seawater (Beardall et al., 2009; Trimborn et al., 2009). However, physical and biochemical

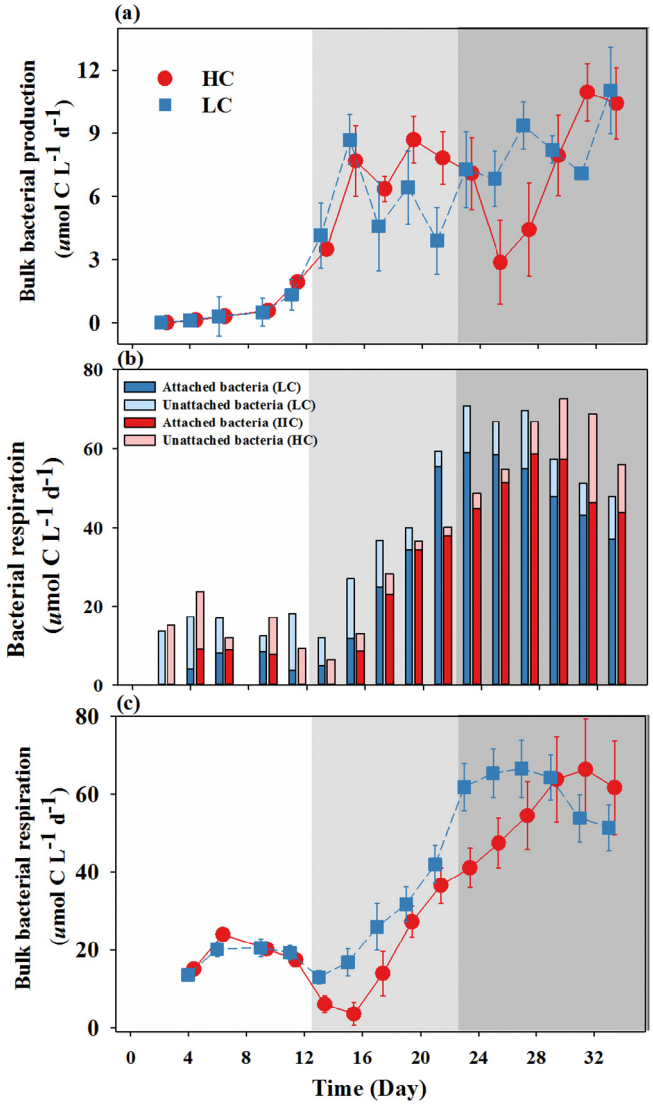

Fig. 3. Temporal variations of (a) bulk bacterial production, (b) respiration of the attached and unattached bacteria (c) bulk bacterial respiration in the high pCO_2 level (HC) and low pCO_2 level (LC) treatments. Style and color-coding as in Fig. 2.

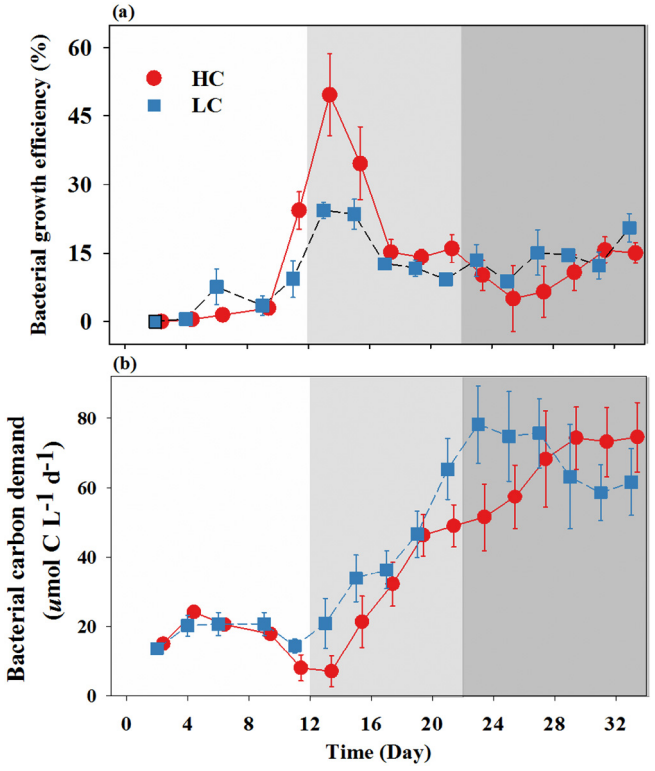

Fig. 4. Temporal variations of (a) bacterial growth efficiency and (b) bacterial carbon demand in the high pCO_2 level (HC) and low pCO_2 level (LC) treatments. Style and color-coding as in Fig. 2.

conditions would change during a real algae bloom, and the function of the CCM in our study may have been constrained by light limitation and the paucity of nitrogen for synthesis of CCM-specific proteins during the stationary phase (Giordano et al., 2005; Cassar et al., 2006). In addition to nutrient limitation (Table 1), the average irradiance in the 2.5-m–deep water column would have been only 8% of the surface irradiance at a chl-*a* concentration of 350 μg L^{-1}, assuming a chl-*a*–specific visible light absorption coefficient of 0.014 m^2 mg^{-1} (Atlas and Bannister, 1980). With CCM activity therefore constrained by lack of light and nitrogen, simple diffusion would have accounted for a relatively large percentage of CO_2 supply. Based on laboratory pH manipulation experiments, Riebesell et al. (1993) have pointed out that the flux of CO_2 to a cell's surface from diffusion depends on many factors, including the CO_2 concentration in the bulk medium, temperature, the cell radius, and the rate of chemical hydration of CO_2 by H_2O. During stationary phase, the CO_2 concentrations in the bulk medium would have played a major role in determining the rate of diffusion of CO_2 through the boundary layer around a cell because other conditions in the two treatments were very similar. The fact that the pCO_2 in the seawater decreased rapidly at the start of the stationary phase (Fig. 1a) reflects the fact that photosynthetic carbon removal was faster than CO_2 dissolution into the seawater, the implication being that the phytoplankton cells became more sensitive to the difference of pCO_2 between the HC and LC treatments. The continuous supply of air containing 1000 μatm CO_2 in the HC treatment would have facilitated phytoplankton carbon uptake by enhancing the diffusion of CO_2 from the bulk medium to the cell surface. Consistent with our observations, Taucher et al. (2015) also found that most of the significant effects of CO_2 enrichment on DIC uptake by two marine diatoms occurred during stationary phase, when the inorganic carbon systems were similar, rather than during the time when the pCO_2 partial pressures were still close to target levels of 400 μatm and 1000 μatm. Another mechanism responsible for these observations may be the allocation of energy savings from the down-regulation of CCMs during log phase of growth to the uptake and storage of nutrients and to the accumulation of intracellular ATP (Spungin et al., 2014). The greater accumulation of resources in the cells grown under HC conditions during the log phase would have made possible higher primary production rates during the subsequent time when nutrients were depleted and resource allocation became critical (Taucher et al., 2015). The prominent impacts during the stationary phase in the present study suggest that interactive effects of CO_2 enrichment with nutrient and light co-limitation could act synergistically to affect marine diatoms and related biogeochemical cycles. This scenario would be especially true in coastal regions when bloom develop in the future high-CO_2 oceans.

4.3. Responses of heterotrophic bacterial metabolism

In contrast to our hypothesis, we did not observe a significant stimulation of bacterial growth and production concomitant with enhanced primary production during stationary phase I (Table 2; Fig. 3a). Because bacteria require inorganic nutrients to grow (Thingstad et al., 2008), nutrient limitation during stationary phase I may have constrained the expected stimulation of bacterial growth and production during this period.

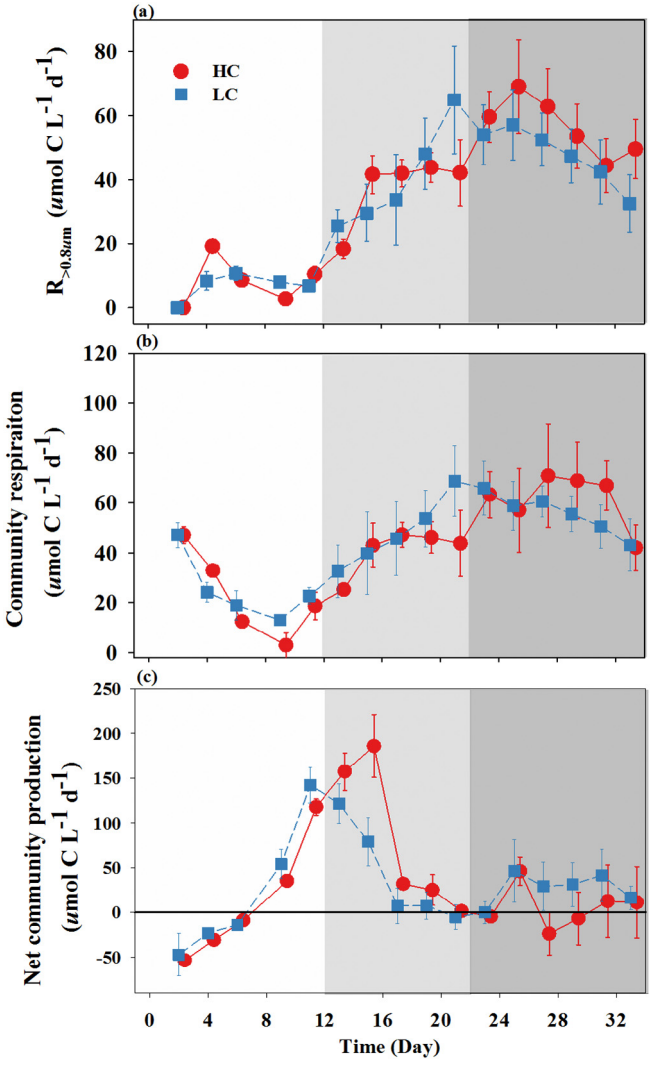

Fig. 5. Temporal variations of (a) Large-size respiration ($R_{>0.8\mu m}$) (b) community respiration and (c) net community production in the high pCO_2 level (HC) and low pCO_2 level (LC) treatments. Style and color-coding as in Fig. 2.

Interestingly, there was a significant increase of BGE and reduction of bulk BR in the HC treatment throughout stationary phase I (Table 2). There have been few direct studies of pCO_2-related effects on bacterial respiration. The effect of increased CO_2 on bacterial respiration was first documented in the laboratory study of Teira et al. (2012), who reported a relatively constant bacterial production but a decline of the respiration rate of *Flavobacteriaceae* grown under a pCO_2 of 1000 μatm. In a natural community dominated by bacteria and picophytoplankton, Spilling et al. (2016) also observed an approximately 40% reduction in community respiration with increasing pCO_2. In contrast, no specific effects on bacterial respiration have been detected by direct measurements in the Artic waters (Motegi et al., 2013). At the present time, the typical pH in ocean surface waters (8.0–8.2) is higher than the intracellular pH (7.4–7.8) of bacteria (Booth, 1985; Padan et al., 2005). The energetic demands associated with this pH gradient include physiological processes such as membrane transport of H^+ or OH^-, enhanced expression of monovalent cation/proton antiporters, and increased acid production to sustain the homeostasis of the internal pH (Smith and Raven, 1979; Padan et al., 2005). A decrease of the pH in seawater due to OA would lead to an external pH closer to the bacterial intracellular pH and thereby reduce the metabolic cost (respiration) associated with internal pH regulation (Teira et al., 2012; Spilling et al., 2016). Organisms require a relatively long time to acclimate to rapid changes of the chemical environment. Although the pH_T during the stationary phase increased to about 8.3 in the two treatments (Fig. 1a), the decrease of BR in the HC treatment may have been related to acclimation to the 12 days of exposure to lower pH during the log phase. The reduction of bulk BR in the HC treatment resulted in a higher BGE and lower BCD (Table 2; Figs. 4a,b), the result being that a higher percentage of assimilated carbon was transformed into bacterial biomass and less was lost to respiration in the HC treatment compared to the LC treatment. The response of BGE during the stationary phase was qualitatively very similar to the effects of elevated pCO_2 on *Flavobacteriaceae* previously reported by Teira et al. (2012), except for the pulse of BGE observed around days 12–14 in the HC (30–55%) and LC treatments (20–30%, Fig. 4a). The BGEs around days 12–14 were much higher than the average values at other time points but within the range of values measured during coastal algae blooms (35–52%, Teira et al., 2015, and 40–60%, García-Martín et al., 2017). The pulse of BGEs was a result of high bulk BP but low bulk BR (Fig. 3a, c), which suggests an uncoupling of production and respiration in the bacteria. This time point was coincident with the peak primary production, and thus the high growth efficiency might be related to the shift of bacterial activity from using carbon resources for cell maintenance to biomass production because of the enhancement of phytoplankton-produced dissolved organic carbon. Overall, the implication of significant increase in BGEs is that transfer of carbon to higher trophic levels through the microbial loop (Azam et al., 1983; Ducklow, 2000) under future OA conditions would be more efficient than is presently the case.

4.4. Responses of community metabolism and implications

We observed a significant (45%) increase of NCP (Table 2; Fig. 5c) during stationary phase I as a result of the enhancement of $GPP_{in\text{-}situ}$ and insignificant changes of CR in the HC treatment. The significant elevation of NCP during stationary phase I suggests that CO_2 enrichment may have a profound impact on the net flux of carbon, with more organic matter accumulation under CO_2-enriched conditions (Fig. 6). Changes of CR were statistically insignificant (Table 2; Fig. 5b) because the lower bulk BR in the HC treatment was offset by the higher rate of PR, which reflected the enhancement of photosynthetic rates by the elevated pCO_2. Although responses of respiration at the community level to CO_2 enrichment were not significant, the complex phenomena that contribute to community respiration have been clearly recorded in this study: there were shifts in the relative proportions of carbon consumption between phytoplankton and bacteria and changes of carbon transfer efficiency within the microbial loop. The implication is that comprehensive studies, especially of heterotrophic activity, will be needed in the future to better elucidate how marine systems change in response to OA.

5. Conclusions

The impacts of CO_2 enrichment on microbial autotrophic and heterotrophic carbon metabolism were evaluated in subtropical coastal mesocosms that were manipulated by continuous bubbling with air containing either 1000 or 400 μatm CO_2. The effect of CO_2 enrichment was to enhance NCP for a period of about two weeks due to the simultaneous responses of both autotrophic and heterotrophic organisms. Our study showed that CO_2 enrichment stimulated primary production and carbon transfer efficiency throughout the microbial loop. Such a stimulation would have profound implications for the carbon cycle. Because coastal regions are especially vulnerable to environmental perturbations such as eutrophication (Borgesa and Gypensb, 2010) and hypoxia (Mucci et al., 2011), their interactions with global ocean acidification may lead to unprecedented complexity.

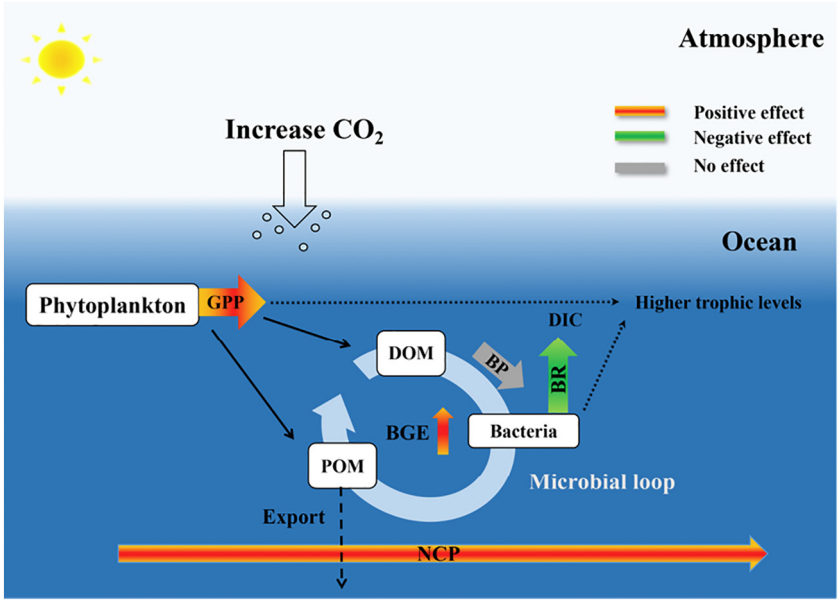

Fig. 6. A schematic illustrating the responses of microbial metabolism under the CO_2 enrichment. According to our findings, rising CO_2 leads to enhanced gross primary production and decline in bacterial respiration. Few effects occur in the bacterial production. Together, these changes increase the net community production at the community level. Additionally, the reduce in the bacterial respiration but constant bacterial production result in an elevation of bacterial growth efficiency, implying with more carbon into bacterial biomass rather than loss in terms of CO_2. GPP: gross primary production. BP: bacterial production. BR: bacterial respiration. BGE: bacterial growth efficiency. NCP: net community production. POM: particulate organic matter. DOM: dissolved organic matter. DIC: dissolved inorganic carbon.

Conflict of interest

The authors declare no conflict of interests.

Acknowledgments

This work was supported mainly by grants from the National Key Research and Development Program (No. 2016YFA0601203) and the China NSF (No. 41330961, U1606404, 41776146, 41720104005). We thank Tifeng Wang, Nana Liu, Futian Li, Peng Jin, Ruiping Huang, Shanying Tong, Xin Lin, and Xiangqi Yi, Xianglan Zeng, whom made contributions to the mesocosm experiments. We also thank Dr. Minhan Dai for providing his unpublished chemical data.

Appendix A. Supplementary data

The graphic of coastal mesocosm (Fig. S1) and methods estimation of in situ photosynthetic rates. Supplementary data to this article can be found online at doi: https://doi.org/10.1016/j.scitotenv.2018.03.222

References

Albright, R., Caldeira, L., Hosfelt, J., Kwiatkowski, L., Maclaren, J.K., Mason, B.M., Nebuchina, Y., Ninokawa, A., Pongratz, J., Ricke, K.L., Rivlin, T., Schneider, K., Sesboue, M., Shamberger, K., Silverman, J., Wolfe, K., Zhu, K., Caldeira, K., 2016. Reversal of ocean acidification enhances net coral reef calcification. Nature 531 (7594):362–365. https://doi.org/10.1038/nature17155.

Atlas, D., Bannister, T., 1980. Dependence of mean spectral extinction coefficient of phytoplankton on depth, water color, and species. Limnol. Oceanogr. 25 (1):157–159. https://doi.org/10.4319/lo.1980.25.1.0157.

Azam, F., Fenchel, T., Field, J.G., Gray, J.S., Meyerreil, L.A., Thingstad, F., 1983. The ecological role of water-column microbes in the sea. Mar. Ecol. Prog. Ser. 10 (3):257–263. https://doi.org/10.3354/meps010257.

Beardall, J., Stojkovic, S., Larsen, S., 2009. Living in a high CO_2 world: impacts of global climate change on marine phytoplankton. Plant Ecology and Diversity 2 (2):191–205. https://doi.org/10.1080/17550870903271363.

Behrenfeld, M.J., Falkowski, P.G., 1997. Photosynthetic rates derived from satellite-based chlorophyll concentration. Limnol. Oceanogr. 42 (1):1–20. https://doi.org/10.4319/lo.1997.42.1.0001.

Booth, I.R., 1985. Regulation of cytoplasmic pH in bacteria. Microbiol. Rev. 49 (4), 359–378.

Borgesa, A.V., Gypensb, N., 2010. Carbonate chemistry in the coastal zone responds more strongly to eutrophication than ocean acidification. Limnol. Oceanogr. 55 (1): 346–353. https://doi.org/10.4319/lo.2010.55.1.0346.

Bunse, C., Lundin, D., Karlsson, C.M.G., Akram, N., Vila-Costa, M., Palovaara, J., Svensson, L., Holmfeldt, K., Gonzalez, J.M., Calvo, E., Pelejero, C., Marrase, C., Dopson, M., Gasol, J.M., Pinhassi, J., 2016. Response of marine bacterioplankton pH homeostasis gene expression to elevated CO_2. Nat. Clim. Chang. 6 (5):483–487. https://doi.org/10.1038/nclimate2914.

Cai, W.J., Dai, M., Wang, Y., Zhai, W., Huang, T., Chen, S., Zhang, F., Chen, Z., Wang, Z., 2004. The biogeochemistry of inorganic carbon and nutrients in the Pearl River estuary and the adjacent northern South China Sea. Cont. Shelf Res. 24 (12):1301–1319. https://doi.org/10.1016/j.csr.2004.04.005.

Cai, W.J., Hu, X., Huang, W.-J., Murrell, M.C., Lehrter, J.C., Lohrenz, S.E., Chou, W.C., Zhai, W., Hollibaugh, J.T., Wang, Y., 2011. Acidification of subsurface coastal waters enhanced by eutrophication. Nat. Geosci. 4 (11):766–770. https://doi.org/10.1038/ngeo1297.

Caldeira, K., Wickett, M.E., 2003. Oceanography: anthropogenic carbon and ocean pH. Nature 425 (6956):365. https://doi.org/10.1038/425365a.

Cassar, N., Laws, E.A., Popp, B.N., 2006. Carbon fractionation by the marine diatom *Phaeodactylum tricornutum* under nutrient- and light-limited conditions. Geochim. Cosmochim. Acta 70 (21):5323–5335. https://doi.org/10.1016/j.gca.2006.08.024.

Coffin, R.B., Montgomery, M.T., Boyd, T.J., Masutani, S.M., 2004. Influence of ocean CO_2 sequestration on bacterial production. Energy 29 (10):1511–1520. https://doi.org/10.1016/j.energy.2003.06.001.

Czerny, J., Schulz, K.G., Ludwig, A., Riebesell, U., 2013. Technical note: a simple method for air–sea gas exchange measurements in mesocosms and its application in carbon budgeting. Biogeosciences 10 (3):1379–1390. https://doi.org/10.5194/bg-10-1379-2013.

Dickson, A., Millero, F.J., 1987. A comparison of the equilibrium constants for the dissociation of carbonic acid in seawater media. Deep-Sea Res. Part I 34 (10):1733–1743. https://doi.org/10.1016/0198-0149(87)90021-5.

Doney, S.C., Fabry, V.J., Feely, R.A., Kleypas, J.A., 2009. Ocean acidification: the other CO_2 problem. Annu. Rev. Mar. Sci. 1:169–192. https://doi.org/10.1146/annurev.marine.010908.163834.

Ducklow, H., 2000. Bacterial production and biomass in the oceans. Microbial Ecology of the Oceans. 1, pp. 85–120.

Dutkiewicz, S., Morris, J.J., Follows, M.J., Scott, J., Levitan, O., Dyhrman, S.T., Berman-Frank, I., 2015. Impact of ocean acidification on the structure of future phytoplankton communities. Nat. Clim. Chang. 5 (11):1002–1006. https://doi.org/10.1038/nclimate2722.

Eppley, R.W., 1972. Temperature and phytoplankton growth in the sea. Fish. Bull. 70 (4), 1063–1085.

Feely, R.A., Alin, S.R., Newton, J., Sabine, C.L., Warner, M., Devol, A., Krembs, C., Maloy, C., 2010. The combined effects of ocean acidification, mixing, and respiration on pH and carbonate saturation in an urbanized estuary. Estuar. Coast. Shelf Sci. 88 (4): 442–449. https://doi.org/10.1016/j.ecss.2010.05.004.

Feng, Y.Y., Warner, M.E., Zhang, Y., Sun, J., Fu, F.X., Rose, J.M., Hutchins, D.A., 2009. Interactive effects of increased pCO_2, temperature and irradiance on the marine coccolithophore *Emiliania huxleyi* (Prymnesiophyceae). Eur. J. Phycol. 43 (1):87–98. https://doi.org/10.1080/09670260701664674.

Gao, K.S., Campbell, D.A., 2014. Photophysiological responses of marine diatoms to elevated CO_2 and decreased pH: a review. Funct. Plant Biol. 41 (5):449–459. https://doi.org/10.1071/FP13247.

Gao, K.S., Zheng, Y.Q., 2010. Combined effects of ocean acidification and solar UV radiation on photosynthesis, growth, pigmentation and calcification of the coralline alga *Corallina sessilis* (Rhodophyta). Glob. Chang. Biol. 16 (8):2388–2398. https://10.1111/j.1365-2486.2009.02113.x.

García-Martín, E.E., Daniels, C.J., Davidson, K., Lozano, J., Mayers, K.M.J., McNeill, S., Mitchell, E., Poulton, A.J., Purdie, D.A., Tarran, G.A., Whyte, C., Robinson, C., 2017. Plankton community respiration and bacterial metabolism in a North Atlantic Shelf Sea during spring bloom development (April 2015). Prog. Oceanogr. (in press). https://doi.org/10.1016/j.pocean.2017.11.002.

Gattuso, J.P., Magnan, A., Bille, R., Cheung, W.W.L., Howes, E.L., Joos, F., Allemand, D., Bopp, L., Cooley, S.R., Eakin, C.M., Hoegh-Guldberg, O., Kelly, R.P., Portner, H.O., Rogers, A.D., Baxter, J.M., Laffoley, D., Osborn, D., Rankovic, A., Rochette, J., Sumaila, U.R., Treyer, S., Turley, C., 2015. Contrasting futures for ocean and society from different anthropogenic CO_2 emissions scenarios. Science 349 (6243), aac4722. https://doi.org/10.1126/science.aac4722.

Giordano, M., Beardall, J., Raven, J.A., 2005. CO_2 concentrating mechanisms in algae: mechanisms, environmental modulation, and evolution. Annu. Rev. Plant Biol. 56: 99–131. https://doi.org/10.1146/annurev.arplant.56.032604.144052.

Del Giorgio, P., Cole, J., 2000. Bacterial energetics and growth efficiency. Microbial Ecology of the Oceans. Wiley-Liss :pp. 289–325. https://doi.org/10.1146/annurev.ecolsys.29.1.503.

Grossart, H.P., Allgaier, M., Passow, U., Riebesell, U., 2006. Testing the effect of CO_2 concentration on the dynamics of marine heterotrophic bacterioplankton. Limnol. Oceanogr. 51 (1):1–11. https://doi.org/110.4319/lo.2006.51.1.0001.

Harris, G.P., Piccinin, B.B., Vanryn, J., 1983. Physical variability and phytoplankton communities. 5. cell-size, niche diversification and the role of competition. Arch. Hydrobiol. 98, 215–239.

Hedges, J.I., Baldock, J.A., Gélinas, Y., Lee, C., Peterson, M.L., Wakeham, S.G., 2002. The biochemical and elemental compositions of marine plankton: a NMR perspective. Mar. Chem. 78 (1):47–63. https://doi.org/10.1016/S0304-4203(02)00009-9.

Hein, M., SandJensen, K., 1997. CO_2 increases oceanic primary production. Nature 388 (6642):526–527. https://doi.org/10.1038/41457.

Hopkinson, B.M., Dupont, C.L., Allen, A.E., Morel, F.M., 2011. Efficiency of the CO_2-concentrating mechanism of diatoms. Proc. Natl. Acad. Sci. U. S. A. 108 (10): 3830–3837. https://doi.org/10.1073/pnas.1018062108.

Iglesias-Rodriguez, M.D., Halloran, P.R., Rickaby, R.E., Hall, I.R., Colmenero-Hidalgo, E., Gittins, J.R., Green, D.R., Tyrrell, T., Gibbs, S.J., von Dassow, P., Rehm, E., Armbrust, E.V., Boessenkool, K.P., 2008. Phytoplankton calcification in a high-CO_2 world. Science 320 (5874):336–340. https://doi.org/10.1126/science.1154122.

Jacoby, J.M., Collier, D.C., Welch, E.B., Hardy, F.J., Crayton, M., 2000. Environmental factors associated with a toxic bloom of *Microcystis aeruginosa*. Can. J. Fish. Aquat. Sci. 57 (1): 231–240. https://doi.org/10.1139/f99-234.

Kerimoglu, O., Straile, D., Peeters, F., 2012. Role of phytoplankton cell size on the competition for nutrients and light in incompletely mixed systems. J. Theor. Biol. 300: 330–343. https://doi.org/10.1016/j.jtbi.2012.01.044.

Kirchman, D., 1993. Leucine incorporation as a measure of biomass production by heterotrophic bacteria. Handbook of Methods in Aquatic Microbial Ecology. Lewis, pp. 509–512.

Laws, E.A., 1991. Photosynthetic quotients, new production and net community production in the open ocean. Deep-Sea Res. I 38 (1):143–167. https://doi.org/110.1016/0198-0149(91)90059-O.

Laws, E.A., Bannister, T.T., 1980. Nutrient- and light-limited growth of *Thalassiosira fluviatilis* in continuous culture with implications for phytoplankton growth in the ocean. Limnol. Oceanogr. 25 (3):457–473. https://doi.org/110.4319/lo.1980.25.3.0457.

Laws, E., Caperon, J., 1976. Carbon and nitrogen metabolism by *Monochrysis lutheri*: measurement of growth-rate-dependent respiration rates. Mar. Biol. 36 (1):85–97. https://doi.org/110.1007/BF00388431.

Legrand, C., Rengefors, K., Fistarol, G.O., Graneli, E., 2003. Allelopathy in phytoplankton -biochemical, ecological and evolutionary aspects. Phycologia 42 (4):406–419. https://doi.org/10.2216/i0031-8884-42-4-406.1.

Li, F., Beardall, J., Collins, S., Gao, K., 2017. Decreased photosynthesis and growth with reduced respiration in the model diatom *Phaeodactylum tricornutum* grown under elevated CO_2 over 1800 generations. Glob. Chang. Biol. 23 (1):127–137. https://doi.org/10.1111/gcb.13501.

Lin, X., Huang, R., Li, Y., Wu, Y., Hutchins, D.A., Dai, M., Gao, K., 2018. Insignificant effects of elevated CO_2 on bacterioplankton community in a eutrophic coastal mesocosm experiment. Biogeosciences 15 (1):551–565. https://doi.org/10.5194/bg-15-551-2018.

Liu, J.W., Weinbauer, M.G., Maier, C., Dai, M.H., Gattuso, J.P., 2010. Effect of ocean acidification on microbial diversity and on microbe-driven biogeochemistry and ecosystem functioning. Aquat. Microb. Ecol. 61 (3):291–305. https://doi.org/10.3354/ame01446.

Liu, X., Huang, B., Huang, Q., Wang, L., Ni, X., Tang, Q., Sun, S., Wei, H., Liu, S., Li, C., 2015. Seasonal phytoplankton response to physical processes in the southern Yellow Sea. J. Sea Res. 95:45–55. https://doi.org/10.1007/s10021-016-9970-5.

Liu, N., Tong, S., Yi, X., Li, Y., Li, Z., Miao, H., Wang, T., Li, F., Yan, D., Huang, R., 2017. Carbon assimilation and losses during an ocean acidification mesocosm experiment, with special reference to algal blooms. Mar. Environ. Res. 129 (1):229–235. https://doi.org/10.1016/j.marenvres.2017.05.003.

Marie, D., Partensky, F., Jacquet, S., Vaulot, D., 1997. Enumeration and cell cycle analysis of natural populations of marine picoplankton by flow cytometry using the nucleic acid stain SYBR Green I. Appl. Environ. Microb. 63 (1), 186–193.

Martínez, I., Casas, P., 2012. Simple model for CO_2 absorption in a bubbling water column. Braz. J. Chem. Eng. 29 (1):107–111. https://doi.org/10.1590/S0104-66322012000100012.

Mehrbach, C., Culberson, C.H., Hawley, J.E., Pytkowicx, R.M., 1973. Measurement of the apparent dissociation constants of carbonic acid in seawater at atmospheric pressure. Limnol. Oceanogr. 18 (1):897–907. https://doi.org/lo.1973.18.6.0897.

Motegi, C., Tanaka, T., Piontek, J., Brussaard, C.P.D., Gattuso, J.P., Weinbauer, M.G., 2013. Effect of CO_2 enrichment on bacterial metabolism in an Arctic fjord. Biogeosciences 10 (5):3285–3296. https://doi.org/10.5194/bg-10-3285-2013.

Mucci, A., Starr, M., Gilbert, D., Sundby, B., 2011. Acidification of lower St. Lawrence estuary bottom waters. Atmosphere-Ocean 49 (3):206–218. https://doi.org/10.1080/07055900.2011.599265.

Mullin, M.M., Sloan, P.R., Eppley, R.W., 1966. Relationship between carbon content cell volume and area in phytoplankton. Limnol. Oceanogr. 11:307–311. https://doi.org/10.4319/lo.1966.11.2.0307.

Oudot, C., Gerard, R., Morin, P., Gningue, I., 1988. Precise shipboard determination of dissolved-oxygen (Winkler procedure) for productivity studies with a commercial system. Limnol. Oceanogr. 33 (1):146–150. https://doi.org/10.4319/lo.1988.33.1.0146.

Padan, E., Bibi, E., Ito, M., Krulwich, T.A., 2005. Alkaline pH homeostasis in bacteria: new insights. Biochim. Biophys. Acta Biomembr. 1717 (2):67–88. https://doi.org/10.1016/j.bbamem.2005.09.010.

Parthasarathy, R., Ahmed, N., 1996. Size distribution of bubbles generated by fine-pore spargers. Journal of Chemical Engineering of Japan 29 (6):1030–1034. https://doi.org/10.1252/jcej.29.1030.

Pierrot, D., Lewis, E., Wallace, D., 2006. MS Excel Program Developed for CO_2 System Calculations. Carbon Dioxide Information Analysis Center. Oak Ridge National Laboratory, US Department of Energy.

Pinckney, J.L., Millie, D.F., Vinyard, B.T., Paerl, H.W., 1997. Environmental controls of phytoplankton bloom dynamics in the Neuse River Estuary, North Carolina, U.S.A. Can. J. Fish. Aquat. Sci. 54 (11), 2491–2501.

Pörtner, H.O., Farrell, A.P., 2008. Ecology. Physiology and climate change. Science 322 (5902):690–692. https://doi.org/10.1126/science.1163156.

Riebesell, U., Wolfgladrow, D.A., Smetacek, V., 1993. Carbon dioxide limitation of marine phytoplankton growth rates. Nature 361 (6409):249–251. https://doi.org/10.1038/361249a0.

Riebesell, U., Schulz, K.G., Bellerby, R.G., Botros, M., Fritsche, P., Meyerhofer, M., Neill, C., Nondal, G., Oschlies, A., Wohlers, J., Zollner, E., 2007. Enhanced biological carbon consumption in a high CO_2 ocean. Nature 450 (7169):545–548. https://doi.org/10.1038/nature06267.

Riebesell, U., Fabry, V.J., Hansson, L., Gattuso, J.P., 2010. Guide to best practices for ocean acidification research and data reporting. Oceanography 22 (8):260. https://doi.org/10.2777/66906.

Riebesell, U., Czerny, J., von Brockeln, K., Boxhammer, T., Budenbender, J., Deckelnick, M., Fischer, M., Hoffmann, D., Krug, S.A., Lentz, U., Ludwig, A., Muche, R., Schulz, K.G., 2013a. Technical note: a mobile sea-going mesocosm system - new opportunities for ocean change research. Biogeosciences 10 (3):1835–1847. https://doi.org/10.5194/bg-10-5619-2013.

Riebesell, U., Gattuso, J.P., Thingstad, T.F., Middelburg, J.J., 2013b. Arctic ocean acidification: pelagic ecosystem and biogeochemical responses during a mesocosm study. (Preface). Biogeosciences 10 (8):5619–5626. https://doi.org/10.5194/bg-10-1835-2013.

Rochelle-Newall, E., Delille, B., Frankignoulle, M., Gattuso, J.P., Jacquet, S., Riebesell, U., Terbrüggen, A., Zondervan, I., 2004. Chromophoric dissolved organic matter in experimental mesocosms maintained under different pCO_2 levels. Mar. Ecol. Prog. Ser. 272: 25–31. https://doi.org/10.3354/meps272025.

Rokitta, S.D., Rost, B., 2012. Effects of CO_2 and their modulation by light in the life-cycle stages of the coccolithophore *Emiliania huxleyi*. Limnol. Oceanogr. 57 (2):607–618. https://doi.org/10.4319/lo.2012.57.2.0607.

Sampaio, E., Lopes, A.R., Francisco, S., Paula, J.R., Pimentel, M., Maulvault, A.L., Repolho, T., Grilo, T.F., Pousão-Ferreira, P., Marques, A., Rosa, R., 2018. Ocean acidification dampens physiological stress response to warming and contamination in a commercially-important fish (*Argyrosomus regius*). Sci. Total Environ. 618:388–398. https://doi.org/10.1016/j.scitotenv.2017.11.059.

Seitzinger, S.P., 1991. The effect of pH on the release of phosphorus from Potomac estuary sediments: implications for blue-green algal blooms. Estuar. Coast. Shelf Sci. 33 (4): 409–418. https://doi.org/10.1016/0272-7714(91)90065-J.

Serret, P., Fernandez, E., Sostres, J.A., Anadon, R., 1999. Seasonal compensation of microbial production and respiration in a temperate sea. Mar. Ecol. Prog. Ser. 187:43–57. https://doi.org/10.3354/meps187043.

Smith, F.A., Raven, J.A., 1979. Intracellular pH and its regulation. Annu. Rev. of Plant Phycol. 30 (1), 289–311.

Smith, D.C., Steward, G.F., Long, R.A., Azam, F., 1995. Bacterial mediation of carbon fluxes during a diatom bloom in a mesocosm. Deep-Sea Res. Part II. 42 (1):75–97. https://doi.org/10.1016/0967-0645(95)00005-B.

Spilling, K., Paul, A.J., Virkkala, N., Hastings, T., Lischka, S., Stuhr, A., Bermudez, R., Czerny, J., Boxhammer, T., Schulz, K.G., Ludwig, A., Riebesell, U., 2016. Ocean acidification decreases plankton respiration: evidence from a mesocosm experiment. Biogeosciences 13 (16):4707–4719. https://doi.org/10.5194/bg-13-4707-2016.

Spungin, D., Berman-Frank, I., Levitan, O., 2014. *Trichodesmium*'s strategies to alleviate phosphorus limitation in the future acidified oceans. Environ. Microbiol. 16 (6): 1935–1947. https://doi.org/10.1111/1462-2920.12424.

Stocker, T., Qin, D., Plattner, G., Tignor, M., Allen, S., Boschung, J., Nauels, A., Xia, Y., Bex, V., Midgley, P., 2013. IPCC, 2013: climate change 2013: the physical science basis. Contribution of Working Group I to the Fifth Assessment Report of the Intergovernmental Panel on Climate Change, of the Intergovernmental Panel on Climate Change, pp. 710–719.

Strathmann, R.R., 1967. Estimating organic carbon content of phytoplankton from cell volume or plasma volume. Limnol. Oceanogr. 12:411–418. https://doi.org/10.4319/lo.1967.12.3.0411.

Taucher, J., Jones, J., James, A., Brzezinski, M.A., Carlson, C.A., Riebesell, U., Passow, U., 2015. Combined effects of CO_2 and temperature on carbon uptake and partitioning by the marine diatoms *Thalassiosira weissflogii* and *Dactyliosolen fragilissimus*. Limnol. Oceanogr. 60 (3):901–919. https://doi.org/10.1002/lno.10063.

Teira, E., Fernandez, A., Alvarez-Salgado, X.A., Garcia-Martin, E.E., Serret, P., Sobrino, C., 2012. Response of two marine bacterial isolates to high CO_2 concentration. Mar. Ecol. Prog. Ser. 453:27–36. https://doi.org/10.3354/meps09644.

Teira, E., Hernando-Morales, V., Fernández, A., Martínez-García, S., Álvarez-Salgado, X.A., Bode, A., Varela, M.M., 2015. Local differences in phytoplankton-bacterioplankton coupling in the coastal upwelling off Galicia (NW Spain). Mar. Ecol. Prog. Ser. 528: 53–69. https://doi.org/10.3354/meps11228.

Thingstad, T.F., Bellerby, R.G., Bratbak, G., Borsheim, K.Y., Egge, J.K., Heldal, M., Larsen, A., Neill, C., Nejstgaard, J., Norland, S., Sandaa, R.A., Skjoldal, E.F., Tanaka, T., Thyrhaug, R., Topper, B., 2008. Counterintuitive carbon-to-nutrient coupling in an Arctic pelagic ecosystem. Nature 455 (7211):387–390. https://doi.org/10.1038/nature07235.

Tortell, P.D., Morel, F.M.M., 2002. Sources of inorganic carbon for phytoplankton in the eastern subtropical and equatorial Pacific Ocean. Limnol. Oceanogr. 47 (4): 1012–1022. https://doi.org/10.4319/lo.2002.47.4.1012.

Trimborn, S., Wolf-Gladrow, D., Richter, K.U., Rost, B., 2009. The effect of pCO_2 on carbon acquisition and intracellular assimilation in four marine diatoms. J. Exp. Mar. Biol. Ecol. 376 (1):17–25. https://doi.org/10.1016/j.jembe.2009.05.017.

Yu, Q., Zhang, T., Cheng, Z., Zhao, B., Mulder, J., Larssen, T., Wang, S., Duan, L., 2017. Is surface water acidification a serious regional issue in China? Sci. Total Environ. 584. https://doi.org/10.1016/j.scitotenv.2017.01.116.

Zhang, H., Byrne, R.H., 1996. Spectrophotometric pH measurements of surface seawater at in-situ conditions: absorbance and protonation behavior of thymol blue. Mar. Chem. 52 (1):17–25. https://doi.org/10.1016/0304-4203(95)00076-3.